PROCEEDINGS, Nineteenth Workshop on Geothermal Reservoir Engineering
Stanford University, Stanford, California, January 18-20, 1994
SGP-TR-147

# CHARACTERIZATION OF SUBSURFACE FRACTURE PATTERNS IN THE COSO GEOTHERMAL RESERVOIR BY ANALYZING SHEAR-WAVE SPLITTING OF MICROEARTHQUAKE SEISMOGRAMS

*Min Lou and Jose A. Rial*

*Wave Propagation Laboratory, Department of Geology*
*University of North Carolina at Chapel Hill, NC27599*

## ABSTRACT

A large number of microearthquake seismograms have been recorded by a downhole, three-component seismic network deployed around the Coso, California geothermal reservoir. Shear-wave splitting induced by the alignment of cracks in the reservoir has been widely observed in the recordings. Over 100 events with body wave magnitude greater than 1.0 from microearthquakes recorded since March of 1992. have been processed. The results show that most events with paths within the critical angle that defines the shear-wave window, display clear shear-wave splitting, and the fast shear waves have predominant polarization directions for most stations. The rose diagrams of fast shear-wave particle motion suggest that there are three predominant fracture strikes (or directions of maximum horizontal stresses) in the Coso geothermal field: *N 40°-60°E*, *N 0°-25°E*, and *N 25°-35° W*, which are consistent with photographically or magnetically mapped alignments on the surface. From the delay time of split shear waves, we estimate that the crack density in the most active geothermal reservoir area (above *3.00km* depth) ranges between *0.030* and *0.055*, values commonly found in other hydrocarbon or geothermal reservoirs.

## 1. INTRODUCTION

Shear-wave splitting due to the alignment of vertical cracks in the crust has been widely observed in a variety of tectonic settings and data gathering experiments; from earthquake recordings to controlled-source seismic data. It has also been recognized that the polarization of the fast split shear wave is usually parallel to the local strike of cracks (or direction of the maximum horizontal stress), and the time delay between fast and slow shear waves is directly related to the intensity of crack-induced anisotropy in the medium (Figure 1; see also Crampin 1987, Crampin and Lovell 1991).

Therefore, the interpretation of shear-wave splitting is an important diagnostic tool to determine the direction and evaluate the bulk density of subsurface fractures in hydrocarbon or geothermal reservoirs (Cliet et al 1991, Muller 1991, Sachpazi and Hirn 1991, Sato et al 1991). We here report on the determination of fracture patterns and crack density in the Coso geothermal field by the above mentioned methods using a large number of microearthquake seismograms recorded by a downhole, three-component seismic network (Malin 1993).

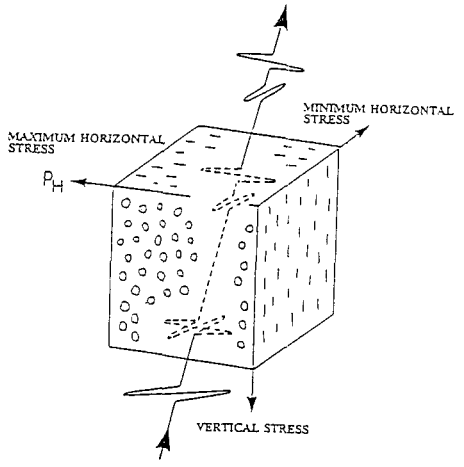


Fig. 1. Schematic illustration of stress-aligned cracks and shear-wave splitting. The cracks are aligned by the typical stress relationships in the subsurface crust. the leading split shear wave is polarized parallel to the strike of cracks (after Crampin 1987).

*Methodology*

Shear-wave splitting is best identified by the examination of polarization diagrams of the two horizontal orthogonal components of shear-wave arrivals. Almost all shear-wave first arrivals are observed to have linear polarization. After a delay of usually hundredths of a second, the first motions are followed by abrupt changes in direction that evolve into elliptical motion, or further linear motion along different polarization directions as the time delay becomes long enough to separate the late signal from the initial arrival (e.g. see Figure 2).

To quantitatively determine the polarization and time delay of split shear waves, the following processing method is used: First, the two horizontal components of the shear wave seismograms are numerically rotated to search for the orientation along which the ratio of the projections of the particle displacement reaches a maximum. In a time window that contains only the fast shear-wave arrival, the azimuth at which this maximum ratio occurs is taken as the polarization direction of fast shear wave (Shih, Meyer and Schneider 1989). Second,

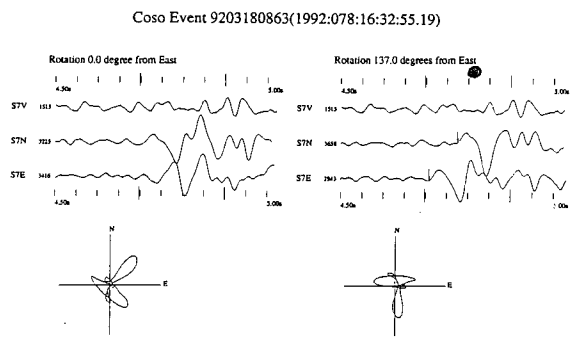


Fig. 2. Shear-wave splitting recorded on station S7, from event 9203180863. The splitting is best detected from the polarization diagram of the horizontal components(S7N, S7E) over a windowed shear-wave train. The polarization direction of the leading shear-wave is about $137^o$ measured counter-clockwise from an assumed East* direction. The two split shear waves (fast and slow) are clearly identified after the seismograms are rotated into the polarization directions corresponding to the fast and slow shear waves.

after the appropriate rotation of the seismogram components to the azimuth angle previously determined has been performed, the time delay between the split shear waves is measured by a standard cross-correlation function.

Although straightforward, the detection and analysis of shear-wave splitting must be based on a large set of shear-wave seismogram data. The behavior of shear-wave splitting above small earthquakes is usually very complicated, because of the complexity of the source signal, subsurface geology structure, and surface topography. One major restriction to the analysis of shear-wave splitting is that, to obtain correct interpretation of split shear-waves, the recording site needs to be within the shear-wave window. The shear-wave window beneath a recording site is defined by the critical angle *arcsin (Vs/ Vp)*. For angles of incidence greater than the critical angle (outside the shear-wave window), shear waves have such interaction with the free surface that almost all similarities with the incoming waveform are irretrievably lost (Booth and Crampin 1985). The critical angle defining the shear-wave window is about $35^o$ in a half space with a Poisson' ratio of *0.25*. However, ray curvature due to low-velocity surface layers usually allows the effective window to be enlarged to angles of incidence of $45^o$ or $50^o$.

## 2. SHEAR-WAVE SPLITTING FROM THE COSO MICROEARTHQUAKE SEISMOGRAMS

The Coso geothermal area is a very active seismic zone with an average of 20 microearthquakes per day; about half of them associated with the geothermal field activity (Malin 1993). Most of these events have been located and cataloged by Peter Malin's seismology group at Duke University. These seismic data offer a unique opportunity to study shear-wave splitting and anisotropy in the reservoir area.

From the numerous Coso microearthquakes recorded since March of 1992, we restricted the shear-wave analysis to those events with body wave magnitudes greater than *1.0*. The analysis was restricted to high signal/noise ratio, clear seismograms, not suspect of complications and presenting an impulsive and short shear-wave signal with shear-wave motion polarized primarily in the horizontal plane, i.e., events with paths within the shear-wave window.

To illustrate, Figure 2 shows a typical example of shear-wave splitting recorded on station S7, from event 9203180863. The splitting is clearly detected on the polarization diagram of the horizontal components. Figure 3 shows the azimuth function, i.e., the ratio of the horizontal components of particle displacement in a time window that contains only the fast shear-wave arrival. From the azimuth function we determine by inspection that the polarization direction of the leading shear-wave is along the azimuth $137^o$ measured counter-clockwise from the East (E*) direction[1]. In Figure 2 the two split shear waves (fast and slow) are clearly identified after the seismograms are rotated so as to coincide with the

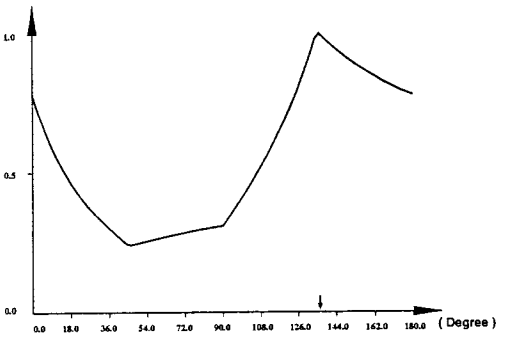


Fig. 3. The polarization direction of the leading shear-wave is found at azimuth $137^o$ measured counter-clockwise from the East* direction, for event 920380863.

polarization directions of the fast and slow shear waves. From the cross-correlation function of these two rotated components we measure the time delay (about 66 ms in this example) at which the maximum in the cross-correlation function occurs (Figure 4). To illustrate the consistency of the results, Figures 5a - b show the shear-wave splitting recorded on the same station S7 as in

[1]This is the East direction in the down-hole instrument frame. The actual, geographical direction of polarization is obtained after correcting for instrument mis-orientation. The correct geographical directions of each station's components are obtained from the polarization of the first arrivals of P-waves from a number of well-located regional microearthquakes. In the following the notation E* is used to indicate (uncorrected) instrumental East direction.

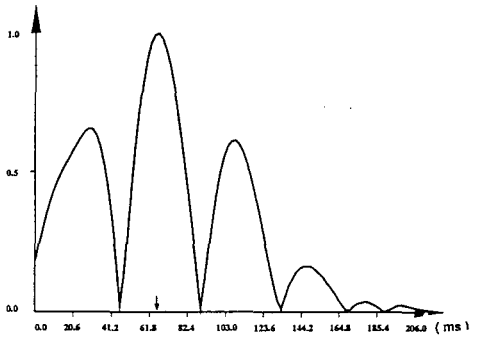


Fig. 4. The cross-correlation function of the two rotated horizontal components (fast and slow) of the seismograms recorded on station S7, from the event 9203180863. The time delay of split shear waves is taken as *66 ms*, at which the maximum of the cross-correlation function occurs.

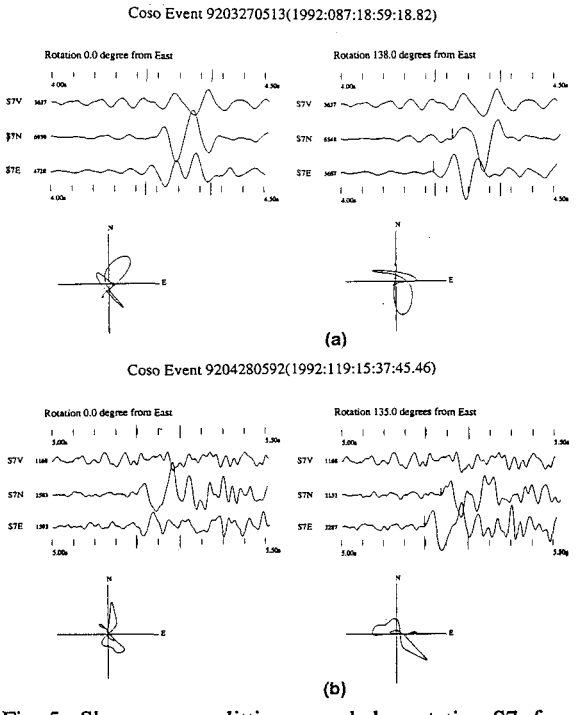


Fig. 5. Shear-wave splitting recorded on station S7, from (a) event 9203270513, and (b) event 9204280592. The polarization directions of the leading shear wave of the two events are about $138^o$ and $135^o$, respectively, measured counter-clockwise from the East* direction. They are almost the same azimuth as the event in Figure 2. The time delays of split shear waves of both events are about *40ms*, which can be easily measured after the two horizontal components of shear waves are rotated into fast and slow shear wave polarization directions.

Figure 2, but from two different events, 9203270513 and 9204280592, which approach the station from different directions. The polarization directions of the leading shear waves for two events are $138^o$ and $135^o$ from the E* direction. Time delays for both events are about *40 ms*. Thus, the polarization directions of the leading shear waves recorded at station S7 are almost the same (within 2 degrees) for all three events. This implies that the observed shear-wave polarizations are not due to the source radiation but the result of crack-induced anisotropic structure between the sources and the station.

Similarly, in Figures 6a -c, we show the shear-wave splitting recorded on a different station, N4, from three different events 9306030128, 93060040151 and 93060040155. We find almost the same polarization direction ($70^o$ measured counter-clockwise from the E* direction in this case) for three events. The time delays of split shear-waves for these three events are *56ms*, *53ms* and *41ms*, respectively.

## 3. RESULTS

We processed and analyzed shear-wave splitting from over 100 microearthquake events around the Coso geothermal area. A catalog containing shear-wave splitting (polarization direction and time delay) and source locations has been assembled. From the catalog of shear-wave splitting, we infer the following information on the strike of fracture (or direction of the maximum horizontal stress) and crack density in the Coso geothermal field:

### (1) STRIKE OF FRACTURES (OR DIRECTION OF THE MAXIMUM HORIZONTAL STRESS)

To infer the local strike of fracture in the Coso area, we have plotted the rose diagrams of the fast shear-wave polarization direction vs frequency for most Coso network stations. Figure 7 shows the rose diagrams of the corrected polarization directions of leading shear wave for eight stations. Almost every rose diagram has a dominant polarization direction, which is here interpreted as the local strike of fracturing or direction of the maximum horizontal stress. Basically, there are three predominant strike groups observed in these rose diagrams: $N\ 40^o$-$60^o\ E$(for stations S2, S7, N5), $N\ 0^o$-$25^o\ E$(for stations S1, S4, S8, N1), and $N\ 25^o$-$35^o\ W$(for station N4). These three predominant fracture trends seem to be generally consistent with the photographically mapped lineaments ($N60^oE$, *N-S*, and $N35^oW$) (Bryan et al. 1990), and magnetically mapped lineaments ( $N40^oE$, *N-S*, and $N55^oW$) (Moore and Erskine, 1990). The Coso surface geology map (Stinson 1977) suggests that the three predominant strikes are related to north and northeast trending faults, as well as northwest trending intrusive dike features.

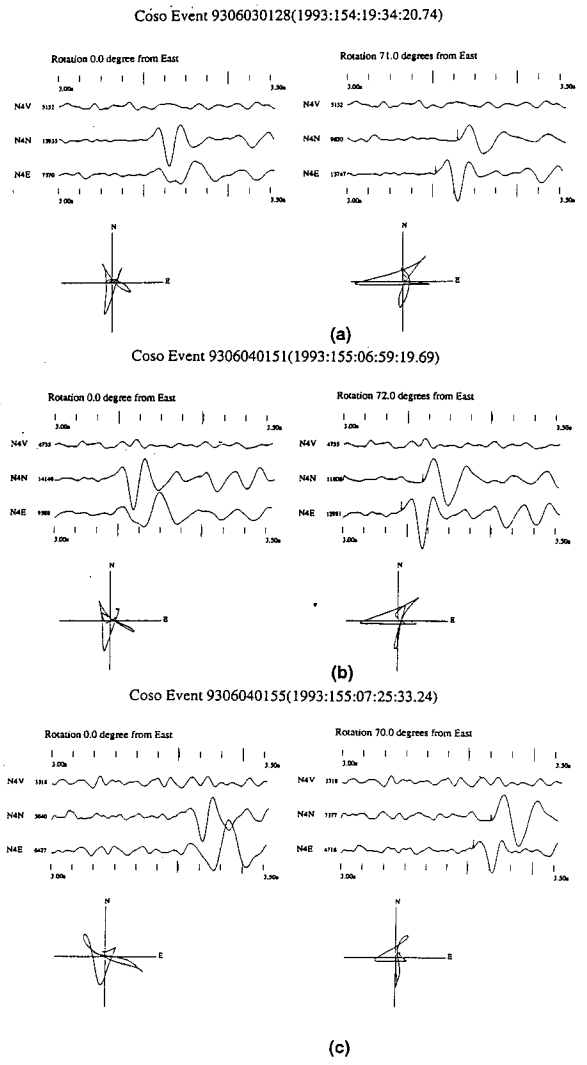


Fig. 6. Shear-wave splitting recorded on station N4, from (a) the event 9306030128, (b) event 93060040151, and (c) event 93060040151. The three events have the almost same polarization direction of the leading shear waves (about $70^o$ measured counter-clockwise from the East* direction). The time delays of split shear waves of these three events are *56ms*, *53ms* and *41ms*, respectively.

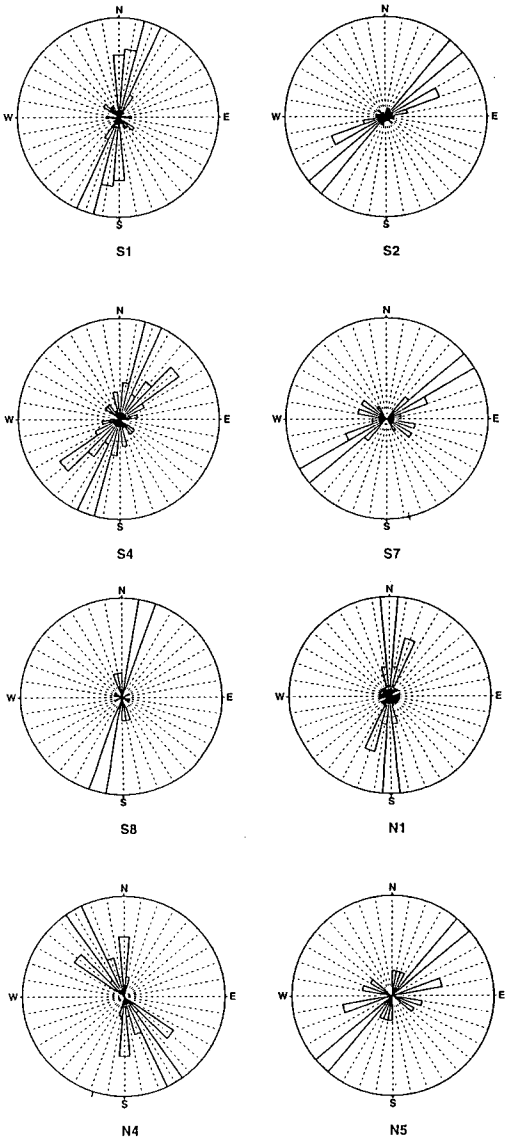


Fig. 7. Rose diagrams of the polarization directions of leading shear waves for the stations S1, S2, S4, S7, S8, N1, N4, and N5 of the Coso seismic network, which show the predominant strike of fractures (directions of the maximum horizontal stress).

## (2) TIME DELAYS OF SPLIT SHEAR WAVES AND CRACK DENSITIES

We have measured the time delays of split shear waves for each processed event. We use the crack density (*CD*) ($CD=Na^3/V$, where $N$ is the number of cracks of average radius $a$ in volume $V$) instead of the time delay to measure the intensity of crack-induced anisotropy in the medium. If we assume that anisotropy is caused by aligned water-filled cracks contained in an otherwise isotropic homogeneous medium, and that each crack is like a thin disk opening radius much smaller than wavelength of shear-waves, then the velocities of two split shear waves can be written (Hudson 1981):

$$V_{SP}^2=\beta^2\,[1 - 8/3\,\varepsilon\,\alpha^2/(3\alpha^2-2\beta^2)\,(cos4\theta +1)] \quad (1)$$

$$V_{SR}^2 = \beta^2 [1 - 8/3\, \varepsilon\, a^2/(3\alpha^2 - 2\beta^2)(\cos 2\theta + 1)] \quad (2)$$

Here $V_{SP}$ and $V_{SR}$ are velocities of quasi- shear waves that are polarized parallel and at right-angle to the plane of incidence, respectively; $\varepsilon$ is crack density (*CD*); $\theta$ is the angle of propagation from the strike of cracks; $\alpha$ and $\beta$ are compressional and shear wave velocities in the isotropic rock matrix, respectively.

The time delay $\tau$ is given by the expression

$$\tau = ( 1/V_{SP} - 1/V_{SR} ) L \quad (3)$$

where $L$ is a propagation distance between source and receiver.

If we assume that the Poission's ratio of the isotropic rock matrix is 0.25, and $\varepsilon << 1$, we have the following approximation relation between $\tau$ and $\varepsilon$ ( Sato et. al., 1991):

$$\tau = 4\varepsilon ( \cos 4\theta - \cos 2\theta ) L / 7\beta. \quad (4)$$

Using the above formulation and the isotropic velocity model in the Coso area (Malin and Erskine 1990, Alvarez 1992), we estimate that the crack density ranges between *0.010* and *0.055* throughout the Coso area, changing with different depths and locations. Statistically, the Coso area seems to be divided into three depth layer groups with different crack densities: For a layer above the depth of *2.50km*, the crack density is between *0.040-0.055*. This crack density is higher than those (<=0.04) commonly found in normally cracked sedimentary, metamorphic, and igneous rocks (Crampin et al. 1986, Crampin and Booth 1985, Robert and Crampin 1986), but since above this depth there is an active geothermal reservoir area, the higher crack density is expected. The crack density in this depth area is also near to that (>=0.05) found in a Japanese geothermal reservoir (Sato, Matsumoto and Nitsuma 1991). For layer depth between *2.50km* and *3.00km*, the crack density ranges between *0.030* and *0.040*. This is a crack density commonly found in a number of hydrocarbon sedimentary reservoir rocks (Crampin et al 1986). For layer depth below *3.00km*, the crack density varies from *0.010* to *0.030*, which is consistent with the known crack density in the crust.

## 4. CONCLUSIONS AND DISCUSSION

Shear-wave splitting induced by the alignment of cracks in the Coso geothermal field has been clearly identified from most events with paths within the critical angle that defines the shear-wave window. The polarization directions of leading shear-waves suggests that there are three predominant fracture strikes around the area: *N 40°-60° E*, *N 0°-25° E*, and *N25°-35°W*, which are generally consistent with photographically or magnetically mapped alignments on the surface. From the delay time of split shear waves, we estimate that the crack density in the most active geothermal reservoir area (above *3.00km* deep) ranges between *0.030* and *0.055*, which is commonly found in other geothermal or hydrocarbon reservoirs. The variation in time delays of split shear waves and crack density observed among different depths and stations in the Coso area suggests that near-station effects may contribute heavily to anisotropy effects. A local stronger near-surface anisotropy may overlie a small deeper crustal anisotropy (Sachpazi and Hirn 1991). It appears necessary to use a tomographic inspection method to delineate those portions of the reservoir having different crack densities by inverting the shear-wave delays of different paths. Shear wave trains contain more information than P-wave trains, and shear-wave splitting is very sensitive to the change of the orientation, distribution, and saturation of fractures in the rockmass. Therefore, any time change in the shear-wave splitting character of the recorded seismograms excited by pumping and injection activities may be used to monitor the production and operation process in the geothermal reservoirs.

## ACKNOWLEDGEMENTS

This research is co-sponsored by the US Navy (Geothermal Program Office, Naval Air Weapons Station, China Lake), Idaho National Engineering Laboratory (EG&G), the California Energy Company, Inc., and the Department of Energy (Geothermal Division), under subcontract No. C93-160437.
We thank Peter Malin for many helpful discussions and suggestions.

## REFERENCES

Alvarez, M.G. (1992) *The seismotectonics of the southern Coso range observed with a new borehole seismographic network*, Master degree thesis, Duke University.

Booth, D.C. and S. Crampin (1985) Shear-wave polarizations on a curved wavefront at an isotropic free-surface, *Geophys. J. R. astr. Soc.*, **83**, 31-45.

Bryan, J.G., E. Baumgrartner, and W. Austin (1990) Remotely sensed controls on heat flow within the Coso geothermal area: implications for further exploration, Coso Field Trip, edited by Moore J. and Erskine M., AAPG EMD **1**, 41-60.

Cliet, Ch., L. Brodov, A. Tikhonov, D. Marin and D. Michon (1991) Anisotropy survey for reservoir definition, *Geophys. J. Int.*, **107**, 417-427.

Crampin, S. (1987) Geological and industrial implications of extensive-dilatancy anisotropy, *Nature*, **328**, 491-496.

Crampin, S. and D.C., Booth (1985) Shear-wave polarization near the North Anatolian Faults. II. Interpretation in terms of crack induced anisotropy. *Geophys. J. Roy. Astr. Soc*, **83**, 75-92.

Crampin, S., I. Bush, C. Naville, and D.B., Taylor (1986) Estimating the internal structure of reservoirs with shear-wave VSPs. The Leading Edge, **5**, 11, 35-39.

Crampin, S and J. Lovell (1991) A decade of shear-wave splitting in the Earth's crust: what does it mean? what use can we make of it? and what should we donext?, *Geophys. J. Int.* **107**, 387-407.

Crampin, S., R. Evens and S.B. Ucer (1985) Analysis of records of local earthquakes: the Turkish Dilatancy Projects (TDP1 and TDP2), *Geophys. J. R. astr. Soc.*, **83**, 31-45.

Hudson, J.A. (1981) Wave speeds and attenuation of elastic waves in material containing cracks, *Geophys. J. R. astr. Soc.*, **64**, 133-150.

Malin, P. (1993), Report on workshop on extensional Process in Coso and Indian Wells Valley Area, July 23, 1993, Duke University.

Malin, P.E. and M.C. Erskine (1990) Coincident P and SH reflection from Basement rocks at the Coso geothermal field, *AAPG Bulletin plus abstracts 1990 San Francisco meeting, June 6 to 8, 1990.*

Moore J. and M. Erskine M (editors) (1990) Coso Field Trip, AAPG EMD 1, 41-61.

Mueller, M.C (1991) Prediction of lateral variability in fracture intensityusing multicomponent shear-wave surface seismic as a precursor to horizontal drilling in the Austin Chalk, *Geophys. J. Int.*, **107**, 409-415.

Robert, G. and S. Crampin (1986) Shear-wave polarization in a Hot Rock geothermal reservoir: Anisotropic effects of fractures, *Int. J. Rock Mech Min. Sci. Geomech. Abstr.* **23**, 291-302.

Sachpazi, M and A. Hirn (1991) Shear-wave anisotropy across the geothermal field of Milos, Aegean volcanic arc. *Geophys. J. Int.*, **107**, 673-685.

Sato, M., N. matsumoto and H. Niitsuma (1991) Evaluation of geothermal reservoir cracks by shear-wave splitting of acoustic emission, *Geothermics,* **20**, 197-206.

Shih, X.R., P. Meyer, P. and J.F. Schneider (1989) An automated, analytical method to determine shear-wave splitting. *Tectonophysics*, **165**, 271-278.

Stinson, M (1970). Geology of the Haiwee Reservoir 15' Quadrangle, Inyo County, California: California Division of mines and Geology, Map Sheet 37.